Kidney International, Vol. 44 (1993), pp. 774–788

Interstitial fibrosis in obstructive nephropathy

ATUL K. SHARMA, S. MICHAEL MAUER, YOUNGKI KIM, and ALFRED F. MICHAEL

Department of Pediatrics, Division of Pediatric Nephrology, University of Minnesota, Minneapolis, Minnesota, USA

Interstitial fibrosis in obstructive nephropathy. Interstitial fibrosis and tubular basement membrane (TBM) thickening are evident within 16 days of unilateral ureteral obstruction (UUO) in the rabbit, and resemble the changes previously reported in hydronephrotic human kidneys. The cortical interstitial volume fraction in this rabbit model at 16 days is 43.3 ± 6.1% (± 1 SD) in UUO kidneys, 4.9 ± 3.1% in contralateral kidneys (CLK), and 2.8 ± 0.8% in kidneys from sham-operated animals (ANOVA, $P < 0.0001$). Immunohistochemically, UUO is associated with increased interstitial collagens I and III, fibronectin, heparan sulfate proteoglycan and tubulointerstitial nephritis antigen. Aberrant collagen expression is also evident as interstitial collagen IV becomes prominent. Focal, peritubular accumulation of collagens I and III also appear to encircle the TBM. These changes are accompanied by an early, transient increase in renal cortical mRNA encoding the α1 monomers of collagens I, III and IV, implicating increased matrix synthesis in the pathogenesis of obstructive nephropathy. *In situ* hybridization localized increased expression of α1(I) and α1(IV) mRNA to cells in the interstitial space, with clusters of α1(I) positive cells associated with dilated tubules, muscular arteries and the periglomerular interstitium.

Chronic urinary tract obstruction is a common cause of end-stage renal disease (ESRD) in children. When obstruction occurs early in gestation, renal dysplasia results [1]. Late gestation or postnatal obstruction can lead to irreversible loss of renal function without evidence of dysplasia and is referred to as obstructive nephropathy. Frequently, these two entities overlap, and together they account for 42% of cases of childhood ESRD [2]. Although irreversible loss of renal function occurs rapidly in models of obstructive nephropathy, there is little experimental work examining the pathogenesis of this injury. Several studies have indicated important interrelationships between measures of interstitial expansion and renal dysfunction in a variety of renal disorders [3]. Morphometric studies of hydronephrotic human kidneys also demonstrate a correlation between tubular epithelial atrophy and the degree of interstitial fibrosis [4, 5].

Herein, we have examined the evolution of these changes in the rabbit model of unilateral ureteral obstruction (UUO), in which interstitial fibrosis and thickening of the tubular basement membrane (TBM) are evident by day 16 of UUO. Our results are consistent with increased production and altered composition of the extracellular matrix (ECM) proteins in the cortical interstitium in this model.

Received for publication January 4, 1993
and in revised form April 26, 1993
Accepted for publication May 24, 1993

Methods

Female New Zealand White rabbits weighing 2.5 to 3.0 kg underwent left ureteral ligation at the ureterovesical junction through a small midline incision as previously described [6, 7]. Sham animals underwent laparotomy with manipulation of the left ureter. Surgical anesthesia was induced with intramuscular Ketamine (50 mg/kg), Acepromazine (0.7 mg/kg), and Xylazine (5 to 8 mg/kg). Following surgery, animals were returned to their cages and fed normal rabbit chow and water *ad libitum*. Procaine penicillin 30,000 U/kg i.m. was administered at the time of surgery and for two days post-operatively. Drinking water containing acetominophen for analgesia was also provided for the same period.

A total of 25 animals were included in these studies. Fourteen underwent left ureteral obstruction and 11 underwent sham laparotomy. Ten rabbits from two litters born on the same day were used for quantitation of cortical interstitial volume. Each of five experimental animals was matched for weight and litter with a sham control. An additional 15 animals were included for immunohistochemistry and RNA isolation. Three groups of five littermates were studied. A group of five animals was sacrificed at 3, at 7, and at 16 days following the initial surgery. In each group, LUO was performed in three and sham operations in the remaining two animals. At the time of sacrifice, animals were again anesthetized and the midline incision re-opened. Urine cultures obtained from the bladder and obstructed ureter were negative in all 25 animals. After harvesting kidney tissue, animals were sacrificed by splitting the diaphragm while under deep anesthesia. This protocol was approved by the University of Minnesota Animal Care Committee.

Quantitation of interstitial volume

Experimental animals and their sham controls were sacrificed after 16 days of left ureteral obstruction (LUO) and their kidneys removed. Obstructed kidneys (LUO), unobstructed contralateral kidneys (CLK), and kidneys from sham-operated animals (Sham) were each cut into five to seven transverse sections 0.5 cm thick. Each transverse section was cut longitudinally three to four times and each resultant strip was transected in the midline. A random number table was then used to select an unbiased sample of five to six tissue pieces distributed throughout the renal cortex for fixation in Zenker's

Table 1. Antisera used for immunohistochemistry

Antisera	Source	Type	Specificity
Collagen I	Southern Biotechnology, Birmingham, AL	goat, affinity purified	collagen I
Collagen III	Southern Biotechnology, Birmingham, AL	goat affinity purified	collagen III
M3F7	Developmental Studies Hybridoma Bank, Bethesda, MD [23]	mouse monoclonal	triple helix, $\alpha 1$ (IV)$_2$ $\alpha 2$ (IV) collagen (placental)
$\alpha 2$(IV) collagen	[24]	sheep	globular domain, $\alpha 2$(IV) collagen
Mab 17	[25]	mouse monoclonal	$\alpha 3$(IV) collagen
Fibronectin	Cappel Research Products, Durham, NC	goat, affinity purified	rabbit fibronectin
Mab 4C7	[26]	mouse monoclonal	laminin A
Mab 4E10	[26]	mouse monoclonal	laminin B1
Mab A7L6	[27]	rat monoclonal	perlecan
Mab A9	[28]	mouse monoclonal	nidogen
Mab A8	[29]	mouse monoclonal	tubulointerstitial nephritis antigen

solution followed by embedding in paraffin. Two micron sections were subsequently cut and stained with periodic acid-Schiff (PAS) and projected using a special projection microscope at 200× magnification onto a 9 × 9 cm grid.

Cortical interstitium was defined as the cortical space which was neither glomeruli, tubules, nor vessels larger than a tubular diameter. The number of grid intersections falling on the cortical interstitium and the whole renal cortex were then counted in a total of 10 fields selected by a predetermined mechanical walk across the cut sections, producing an estimate of the volume fraction (Vv) of the cortex which is interstitium (Vv Int/Cortex) [8]. Specimens for electron microscopy (EM) were fixed in glutaraldehyde, treated with osmium tetroxide and embedded in epon.

Immunohistochemistry

A group of five littermates was sacrificed at each time (that is, 3, 7, and 16 days following the initial surgery). Prior to nephrectomy, a cortical wedge biopsy was taken and snap frozen in isopentane pre-cooled in liquid nitrogen for *in situ* hybridization studies. Following nephrectomy, the upper and lower poles were removed and snap frozen directly in liquid nitrogen after medullary tissue was dissected away. These specimens of renal cortex were subsequently processed for renal cortical RNA (*vide infra*). Additional renal tissue was snap frozen in isopentane for immunohistochemistry or was prepared for light microscopy as described above.

Cryostat sections (4 μ) of the frozen biopsy tissue were cut onto glass slides in a constant temperature (25°) and humidity (30%) room and fixed in acetone as previously described [9]. Sections were then incubated for 30 minutes at room temperature with the primary antibodies listed in Table 1. These antisera were selected on the basis of reactivity with the principle collagenous (collagens I, III, and IV), noncollagenous glycoprotein (fibronectin, laminin, nidogen) and proteoglycan (heparan sulfate proteoglycan) components of the cortical interstitium and TBM [10, 11]. After washing with phosphate buffered saline (PBS), fluorescein isothyiocyanate (FITC) conjugated and affinity-purified secondary antisera were applied for 30 minutes: rabbit anti-goat IgG (Pel-Freez, Rogers, Arkansas, USA), goat anti-mouse IgG (Caltag, San Francisco, California, USA), goat anti-rat IgG (Pel-Freez), and rabbit anti-sheep IgG (Pel-Freez). All secondary antisera were preabsorbed with normal rabbit serum prior to use. To retard fluorescent quenching, p-phenylene-diamine was applied in glycerol PBS [12]. Control sections from each animals were incubated with the secondary antisera alone to exclude non-specific reactivity. Sections were examined by indirect immunofluorescence using a Zeiss epifluorescence microscope fitted with appropriate filters (Carl Zeiss Inc., Oberkochen, Germany). Sections from each kidney were graded by two independent observers (AS and YK) for each primary antibody on a scale of 0 to 3+ (0 = absent; + = weakly present; ++ = present; +++ = strongly present). Grading reflected both the intensity and the extent of reactivity. In general, an increase was defined as a change in scale of at least one unit (that is, 0 to + or + to ++). Both interobserver and within-group interanimal variability were minimal.

RNA isolation and hybridization

Renal cortical RNA was isolated from each of 15 animals as described above using 0.2 g of cortical tissue and the single-step acid phenol extraction method of Chomcynzki and Sacchi [13]. The optical density ratio at 260 and 280 nm was consistently ≥ 1.7. The concentration of RNA so isolated was calculated on the basis of absorbance at 260 nm measured on two separate occasions with mean of the two values used as the final datum point. For Northern blots, 20 μg of cortical RNA per kidney was run in 1% agarose denaturing gels with 2.2 M formaldehyde, and transferred electrophoretically to cationic nylon membrane (Boerhinger-Mannheim, Indianapolis, Indiana, USA). An additional lane with 10 μg of total cellular RNA from cultured human mesangial cells was used as a positive control for each Northern gel. For dot blot analysis, each RNA sample was dotted onto the same nylon in 2.5, 1.25, 0.6 and 0.3 μg serial dilutions in a buffer containing 6 × SSC, 7.4% formaldehyde (1 × SSC = 150 mM NaCl, 15 mM sodium citrate, pH 7.0). RNA was fixed to the membrane by ultraviolet crosslinking (Stratalinker, Stratagene, La Jolla, California, USA) or baking at 80°C in a vacuum oven for two hours. Blots were then prehybridized at 42°C for at least six hours. Prehybridization solution contained 50% deionized formamide, 5 × SSC, 10 ×

Denhardt's solution (1 × = 0.02% Ficoll 400, 0.02% polyvinylpyrrolidone, 0.02% bovine serum albumin) 50 mM $NaPO_4$, 1 mg/ml salmon sperm DNA and 0.1% SDS. Hybridization solution containing labeled probe in 50% deionized formamide, 5 × SSC, 2 × Denhardt's solution, 50 mM $NaPO_4$, 100 μg/ml yeast tRNA, 100 μg/ml salmon sperm DNA, and 0.1% SDS was then used to hybridize at 42°C overnight. Stringent washing in 0.2 × SSC, 0.1% SDS at 60°C was followed by autoradiography at −80°C with Kodak XAR intensifying screens. Exposure times varied from overnight to five days.

cDNA probes and quantitation

RNA hybridization studies were performed with cDNA probes encoding the α1 monomers of collagen I (Hf-677) [14], collagen III (Hf-934) [15] and collagen IV (p1275) [16]. The 1.5 kB Eco R1 fragment of Hf-677 was purified from 1% agarose by silica glass affinity (Gene Clean™, Bio 101, La Jolla, California, USA) and subcloned into the Bluescript plasmid vector (Stratagene, La Jolla, California, USA). The 0.7 kB Eco R1-Hind III fragment of Hf-934 was also subcloned into Bluescript. Clone p1275 [α1 (IV)] was used without further modification. In each case, after appropriate restriction enzyme digestion, the cDNAs were separated by agarose gel electrophoresis and purified with the Gene Clean™ reagents. Fifty nanograms of purified cDNA was labeled using the random priming method (Boehringer-Mannheim) with ^{32}P-dCTP (3000 Ci/mmol, I.C.N., Irvine, California, USA). Probe specific activity of 10^9 CPM/μg could be routinely obtained in this fashion. The labeled probe was added to hybridization solution at a concentration of 1 × 10^6 incorporated CPM/ml of solution, where incorporation was assessed by precipitation with trichloracetic acid.

After autoradiograms were developed, the optical densities (O.D.) of individual dots were quantitated using a computer assisted densitometer [17]. The mean O.D. of each dot was then plotted against the amount of RNA blotted onto the membrane and the slope of the best fit regression line ($r > 0.9$ for at least 3 points) was used to determine the relative abundance of the mRNA being studied [18, 19]. Thus, each kidney provided one measurement of mRNA abundance for statistical analysis. To control for loading errors, blots were subsequently re-probed with a cDNA probe encoding the rat 28S ribosomal RNA [20]. For each sample, the slope of the best-fit regression line was then used to normalize the collagen mRNA data. At each time, the mean of the CLK samples was normalized to a value of 1.0, and other values adjusted accordingly.

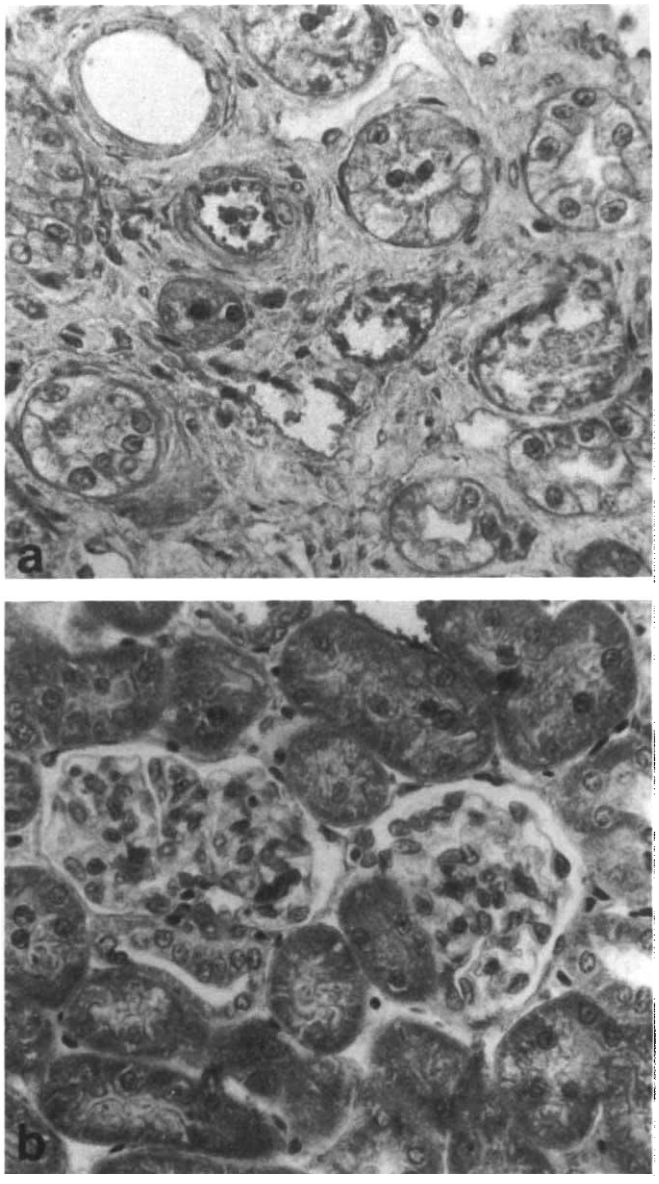

Fig. 1. *Photomicrograph of renal cortex from a kidney obstructed 16 days prior to sacrifice (a) compared with a sham-operated animal (b).* Note the interstitial fibrosis is indicated by blue staining of the interstitium in the obstructed kidney. × 250, trichrome stain.

In situ *hybridization*

In situ hybridization studies were performed using riboprobes generated from the 1.5 kB α1(I) cDNA to localize the origin of increased α1(I) mRNA. Localization of α1(IV) mRNA was with riboprobes encoding the noncollagenous (NC1) domain of human α1(IV), known to be 96% homologous to the corresponding rabbit sequence [21]. This cDNA clone was obtained by polymerase chain reaction (PCR) with the following primers: TCCT TACGACATCATCAAAGGGGA (upstream, primer) and AGAGGATCCTTATGTTCTTCTCATACA (downstream primer). The template for this reaction was a commercial human fetal kidney cDNA library (Clonetech, Palo Alto, California, USA). Reaction conditions were 94° denaturation, 55° annealing, and 72° extension for 40 cycles. PCR consistently yielded a single product of the expected size (1 kB), which was cloned into the Bluescript vector using the Bam H1 site in the 5′ end of the downstream primer. The identity of this cDNA was confirmed by sequencing by the dideoxy chain termination method. The Bluescript plasmids with insert were linearized with appropriate restriction enzymes, purified by gel electrophoresis followed by the Gene Clean™ procedure, and labeled with either T7 or T3 RNA polymerase to produce sense and antisense riboprobes. Probes were labeled with digoxigenin-UTP following the recommended procedures included with the Genius 4 RNA labeling kit (Boehringer Mannheim). The single-stranded RNA probes were then hydrolyzed by incubation for 30 minutes at 60° in 40 mM $NaHCO_3$, 60 mM Na_2CO_3 (pH 10.2). Following alkali hydrolysis and ethanol precipitation, gel electrophoresis

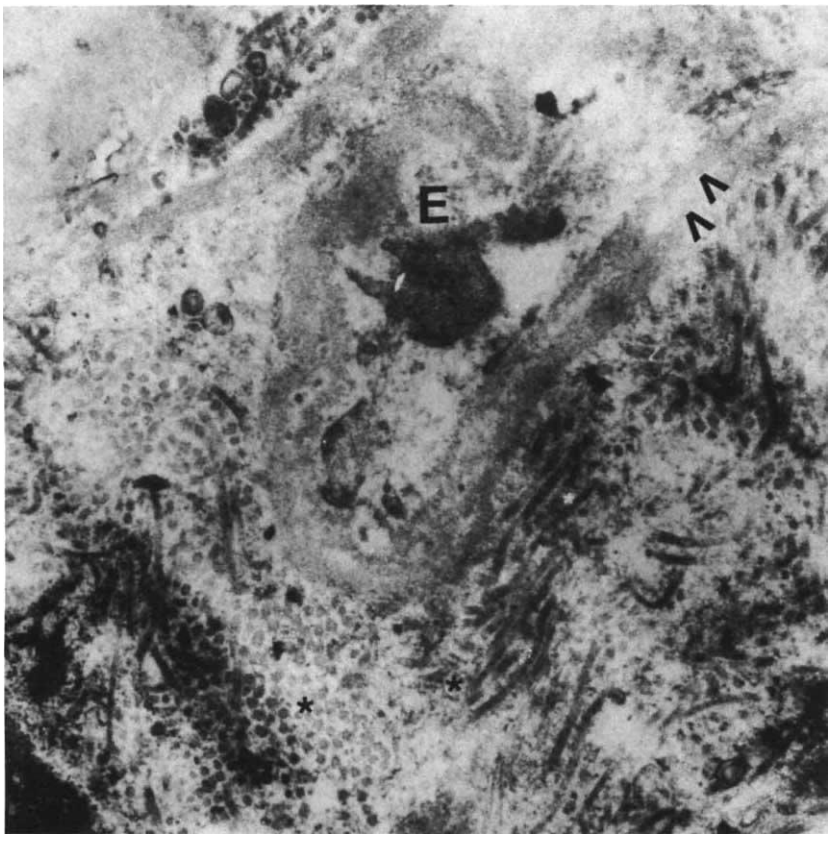

Fig. 2. *Electron micrograph of renal cortex from a kidney obstructed 16 days prior to sacrifice.* The expanded interstitial space (*) contains fibrillary material, and laminations of the tubular basement membrane (arrows) are seen. The tubular epithelial cell (E) has lost its mitochondria and basolateral interdigitations. × 40,000.

demonstrated a smear between 100 to 300 bp, deemed to be the optimal probe size for tissue penetration [22].

For *in situ* hybridization, 8 μ cryostat sections were cut on gelatin subbed slides. Both prehybridization and hybridization were performed in 50% formamide, 1 × Denhardt's solution, 2 × SSC, 0.5% SDS, 250 μg/ml herring sperm DNA, 250 μg/ml yeast tRNA, 10 mM Tris HCl, pH 7.5, 5 mg/ml sodium pyrophosphate, and 10% Dextran sulfate. After prehybridization for one hour at room temperature, hybridization solution containing 300 ng/ml of either the sense or antisense probe was applied to the sections, which were then covered with parafilm and allowed to hybridize at 42 to 46° overnight. The next day, the slides were washed in 2 × SSC, incubated for 30 minutes in 100 μg/ml RNAase A to remove unbound probe, and stringently washed in 0.1 × SSC at 42°. The slides were then blocked with 10% normal goat serum in 150 mM NaCl, 100 mM Tris HCl, pH 7.5 for one hour and incubated in the same solution containing a 1:500 dilution of sheep anti-digoxigenin alkaline phosphatase conjugate for three hours (Boehringer Mannheim). The nitroblue tetrazolium (NBT) color detection reaction was then performed according to the manufacturers instructions (Genius 3 kit, Boehringer Mannheim). The color detection reaction was monitored microscopically and interrupted after four to nine hours by washing in 10 mM Tris, 1 mM EDTA. Sections were then mounted in glycerine and coverslips applied.

Data analysis

The mean Vv Int/Cortex in the LUO, CLK and kidneys from sham-operated controls were compared by factorial analysis of variance (ANOVA) on a MacIntosh personal computer with Statview 4.0 (Abacus Concepts Inc., Berkely, California, USA). The mean mRNA contents of LUO, CLK and Sham groups at each time were similarly compared. When significant differences were noted between the three groups ($P < 0.05$) by ANOVA, post-hoc pairwise comparisons were performed using Fischer's protected least significant difference (PLSD) ($P > 0.05$ = NS). Data are expressed as mean ± standard deviation.

Results

Light and electron microscopy

Interstitial fibrosis was evident within 16 days of LUO (Fig. 1A). By electron microscopy (Fig. 2), the interstitial space was packed with disorganized fibrils. In addition, focal laminations of the TBM were seen. In the kidneys from Sham animals (not shown), the interstitial space was small and contained ordered fibrils; laminations of the TBM were absent. Vv Int/Cortex was 43% in the LUO renal cortex compared with 4.9% in the CLK cortex and 2.8% in kidneys from sham-operated animals 16 days after the initial surgery (Fig. 3; ANOVA, $P < 0.0001$; for the LUO vs. CLK, $P < 0.0001$ by PLSD; for the LUO vs. Sham, $P < 0.0001$; for the CLK vs. Sham, P = NS).

Immunofluorescence microscopy

The results of qualitative immunohistochemistry of both the cortical interstitium and TBM are summarized in Table 2. The TBM and interstitium were graded separately. Collagens I and III were restricted to the interstitial space in the CLK and

Table 2. Immunofluorescence of obstructed and control kidneys (Day 16)

Specificity	Interstitium			TBM		
	Sham	CLK	LUO	Sham	CLK	LUO
Collagen I	+		+	0	0	++[a]
Collagen III	+	+	+++	0	0	++[a]
Collagen IV (helix)	0[b]	0[b]	+++	+++	+++	+++
α2 (IV)	0[b]	0[b]	++	+++	+++	+++
α3 (IV)	0	0	0	+	+	+
Fibronectin	+−++	+−++	+++	0	0	0
Laminin B1	0	0	0	+	+	+
Laminin A	0	0	0	+	+	+
T.I.N. antigen	0−+	0−+	+	+++	+++	+++
Nidogen	0[b]	0[b]	0[b]	++	++	++
Perlecan	0−+	0−+	+	++	++	++

Abbreviations are: TBM, tubular basement membrane; LUO, left ureteral obstruction; CLK, contralateral kidney; Sham, kidney from sham-operated animal.

[a] Focal, peritubular accumulation of collagens I and III were seen in the LUO, likely reflecting interstitial matrix in close proximity to the phase-dense TBMs

[b] Absent in the interstitium except in capillary basement membranes

kidneys from sham-operated animals (Figs. 4 and 5). TBMs reacted strongly with collagen IV antisera, but, with the exception of the peritubular capillary basement membranes, collagen IV was not detectable in the normal interstitium (Figs. 6 and 7). In kidneys from Sham animals and CLK kidneys, fibronectin was restricted to the interstitium (Fig. 7). Laminins A and B1 and nidogen reacted strongly in TBM, but were not present in the interstitium, with the exception of nidogen staining of capillary basement membranes. Perlecan and tubulointerstitial nephritis antigen were present in the TBM and weakly reactive in the interstitial space.

With obstruction, the fibrillary collagens I and III appeared to be diffusely increased in the interstitium at days 7 and 16. There were also focal, peritubular accumulations of collagens I and III encircling the phase-dense TBM (Figs. 4 and 5). The presence of collagen IV reactivity in the interstitial space was visible as early as day 3 of LUO and became more prominent at the later times (Figs. 6 and 7). This expression appeared to be selective for the classical collagen IV network [α1(IV) and α2(IV)], since there was no staining in the interstitium for α3 (IV) (Fig. 7) in any of the animals studied. Interstitial fibronectin reactivity was also increased (Fig. 7) following LUO, evident as early as day 7. The distributions of laminin and nidogen did not change with obstruction, while tubulointerstitial nephritis antigen and Perlecan fluorescence staining was mildly increased in the interstitial space.

RNA studies

RNA hybridization studies were performed using cDNAs encoding the α1 monomers of collagens I, III and IV. Northern blot of RNA from the LUO kidneys and CLK of two day 7 animals demonstrated an increase in α1 (I) collagen mRNA at 4.8 kB with LUO (Fig. 8A). Dot blot analysis of α1 (I) mRNA (Fig. 8B) demonstrated a marked increase at both day 3 and day 7 of LUO. The mRNA contents corrected for the abundance of the 28S ribosomal RNA of the LUO, CLK and kidneys from sham-operated animals are depicted in Figure 8C. All values have been normalized to the CLK value at that time. There were significant group effects at days 3 and 7 of LUO (ANOVA, $P < 0.0001$). At both times, significant differences were found

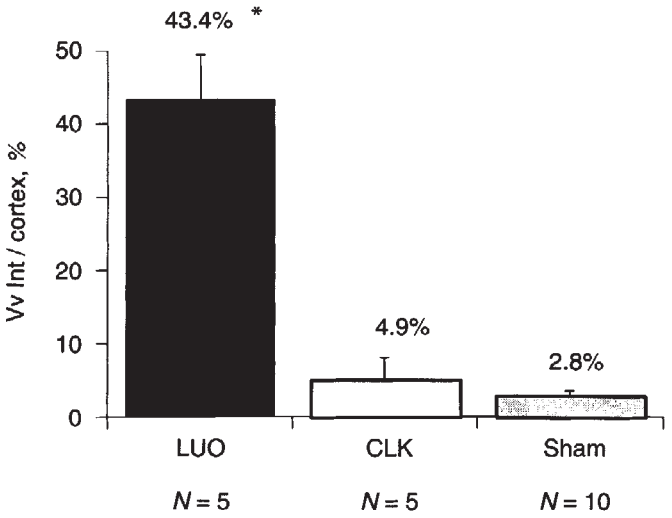

Fig. 3. *Cortical interstitial volume fraction (Vv Int/Cortex) 16 days after the initial surgery in left ureteral obstruction (LUO), contralateral kidneys (CLK), and kidneys from sham-operated animals (Sham).* ANOVA, $P < 0.0001$.

between LUO and CLK ($P < 0.0001$) and LUO and Shams ($P < 0.0001$), but not between the Shams and CLK. α1(I) collagen mRNA in the LUO kidneys was 16.9 ± 3.1 times the CLK at day 3 and 21.6 ± 2.7 times the CLK at day 7, but by day 16 had decreased to 2.4 ± 1.7 times the CLK and was no longer significant.

Similar results were seen with cortical α1 (IV) collagen mRNA (Fig. 9A). The predominant mRNA isoform in both the rabbit and the human control was at 6.8 kB with smaller isoforms at around 5 kB. The abundance of α1(IV) mRNA in each of the experimental groups (LUO, CLK, Sham) was assessed by dot blot (Fig. 9B) at days 3, 7 and 16. Again, there were significant group effects at days 3 and 7 (ANOVA, $P < 0.0001$). Type IV collagen mRNA in the LUO kidneys was increased to 5.8 ± 1.3 times the CLK at day 3 and 6.4 ± 0.7 times the CLK at day 7 (Fig. 9C). At both times, LUO values were significantly different from both CLK and Shams ($P <$

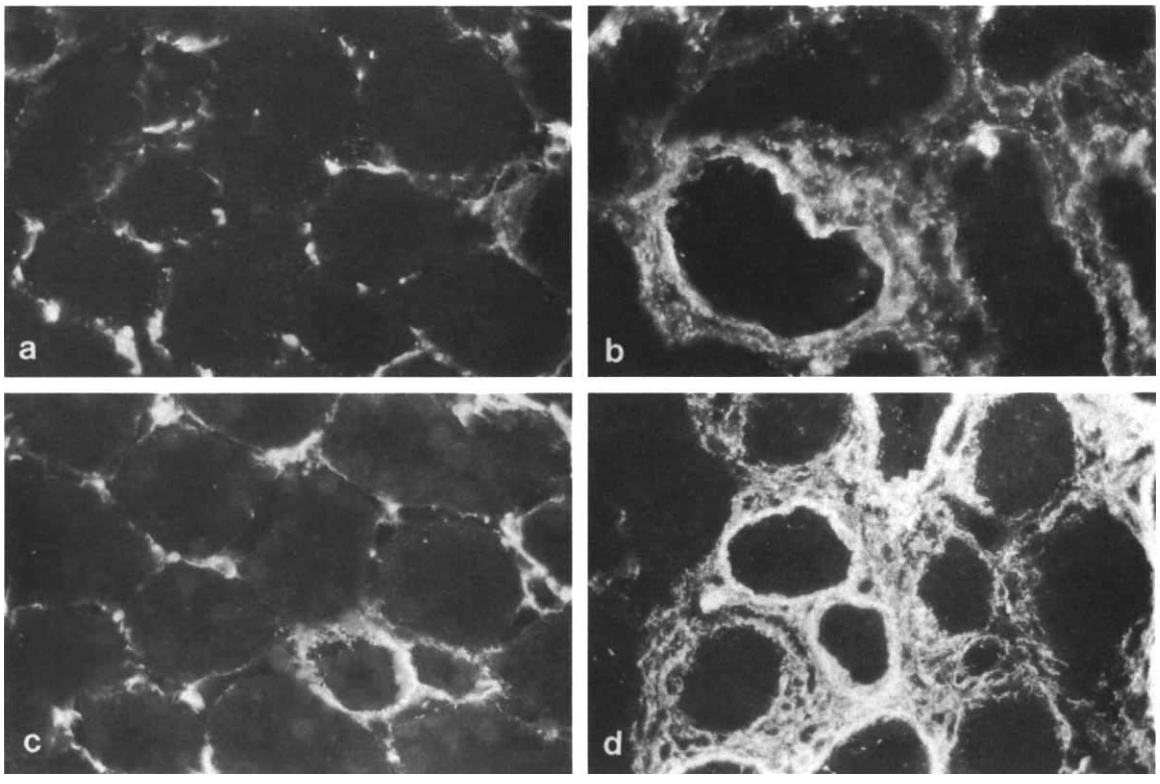

Fig. 4. *Indirect immunofluorescence (400×) with collagen I antisera demonstrating increased reactivity in the expanded interstitium of the obstructed kidney (LUO) when compared with the sections from the kidney of sham-operated animals (Sham).* In addition, focal peritubular accumulations of collagen I appear to encircle the TBM: **(A)** Day 16 Sham; **(B)** Day 16 LUO; **(C)** Day 7 Sham; **(D)** Day 7 LUO.9

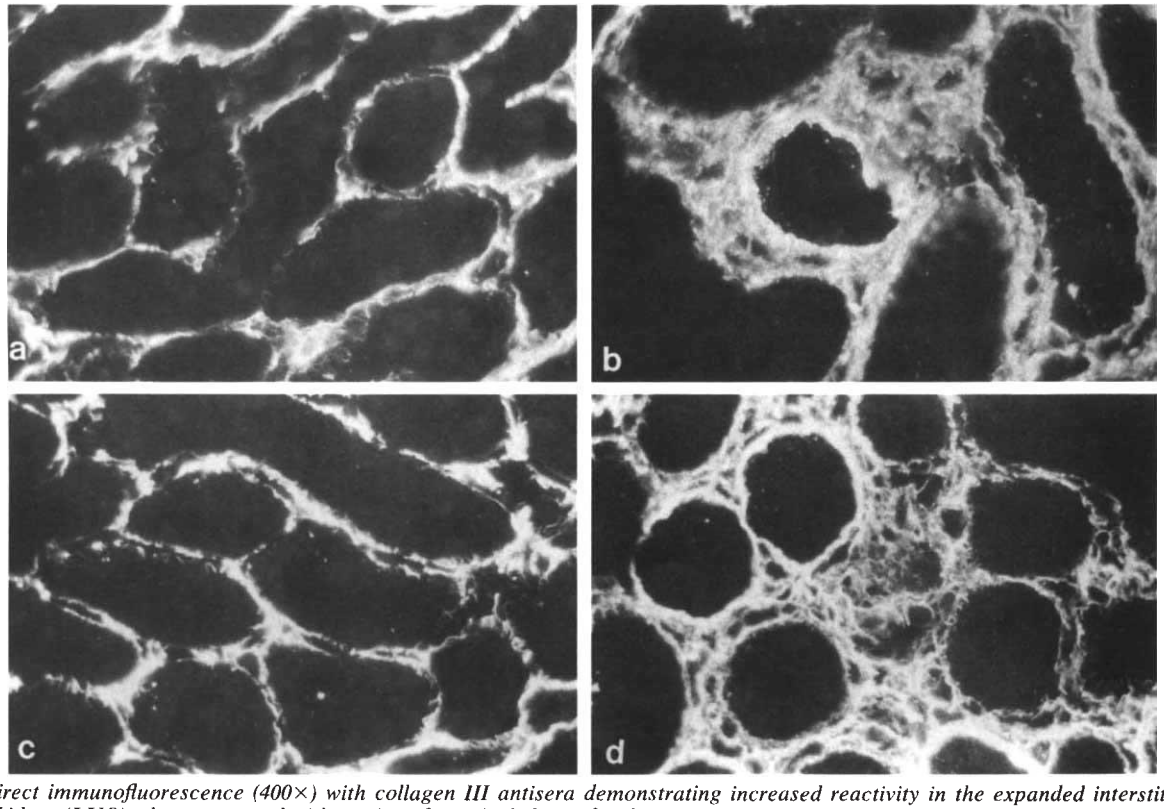

Fig. 5. *Indirect immunofluorescence (400×) with collagen III antisera demonstrating increased reactivity in the expanded interstitium of the obstructed kidney (LUO) when compared with sections from the kidney of a sham-operated animal (Sham).* As was the case for collagen I, there are focal areas where collagen III reactivity appears to encircle the TBM: **(A)** Day 16 Sham; **(B)** Day 16 LUO; **(C)** Day 7 Sham; **(D)** Day 7 LUO.

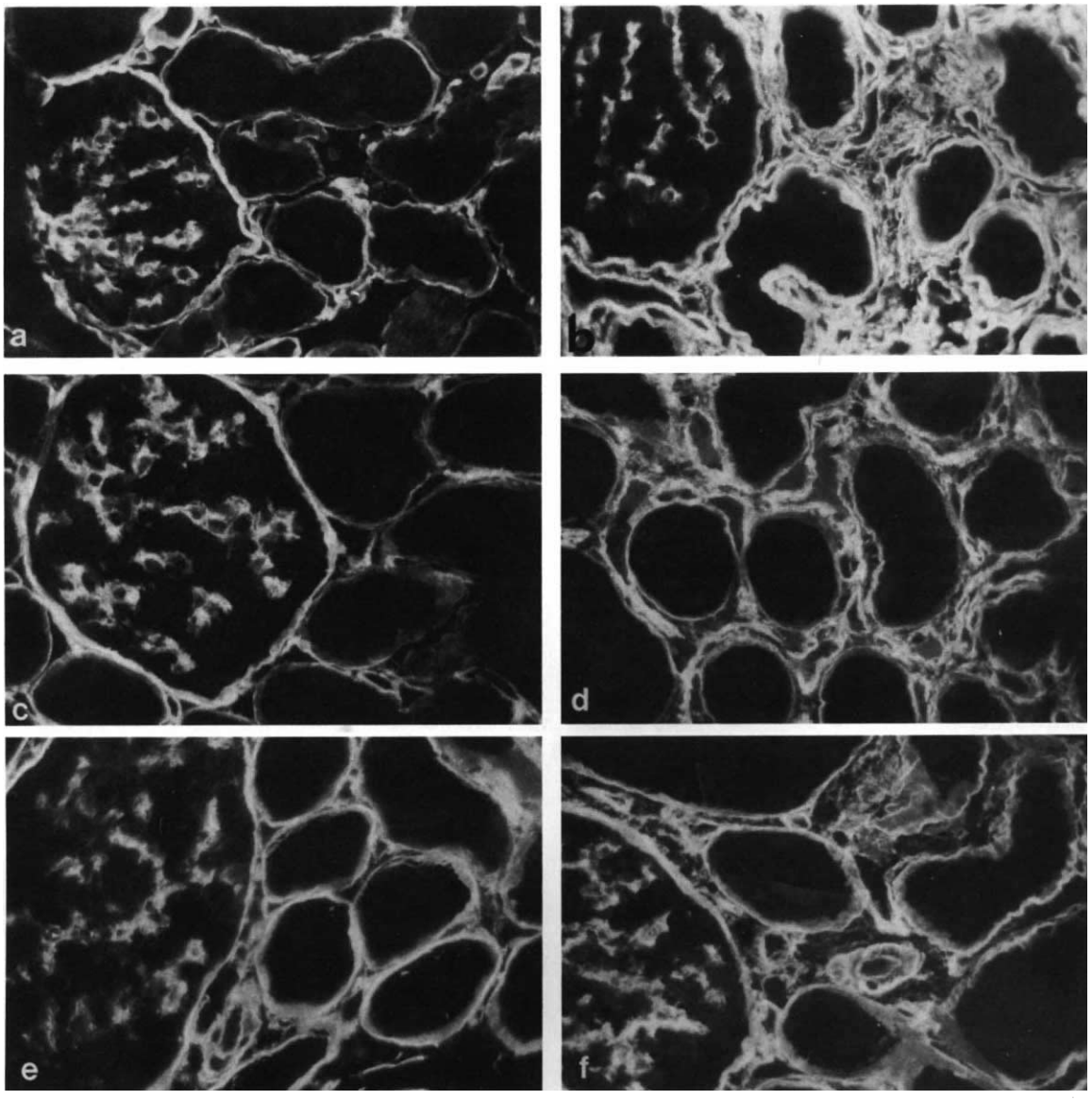

Fig. 6. *Indirect immunofluorescence (400×) with monoclonal antibody M3F7 identifying the triple helix of classical collagen IV.* In the interstitium of the kidney from a sham-operated animal (Sham), collagen IV is seen only in capillary basement membranes. Note the prominence of interstitial collagen IV in the obstructed kidney (LUO): **(A)** Day 16 Sham; **(B)** Day 16 LUO; **(C)** Day 7 Sham; **(D)** Day 7 LUO; **(E)** Day 3 Sham; **(F)** Day 3 LUO.

0.0001) with no significant difference between Sham and CLK kidneys. By day 16, type IV collagen mRNA expression had returned to a value not statistically different from that of the controls.

The specificity of the α1(III) probe is demonstrated by Northern analysis (Fig. 10A). After normalization of the dot blot data to 28S, significant group effects were detected at day 3 and day 7 (Fig. 10B). In the LUO, collagen III mRNA was 5.2 ± 0.6 times the CLK at day 3 (ANOVA, $P < 0.001$) and significantly different from both the CLK and Sham values (LUO vs. CLK, $P < 0.001$; for LUO vs. Sham, $P < 0.002$; for CLK vs. Sham, $P = 0.04$). At day 7 of obstruction, α1 (III) collagen mRNA was 1.6 ± 0.4 times the CLK (ANOVA, $P = 0.04$), but post-hoc testing localized this difference to the comparison of LUO and Sham specimens ($P < 0.02$). At day 16 of UUO, group differences in α1 (III) collagen mRNA expression were no longer detectable.

In situ *hybridization*

Studies were performed on cryostat sections of the LUO and CLK kidneys of two animals sacrificed seven days following UUO because this was the time of maximal expression of α1(I) and α1(IV) mRNA. Signal could be detected with the antisense probe in the LUO cortex after as little as two hours of color detection, although the reaction was allowed to continue for four to nine hours. Cells staining positively for α1(I) were exclusively interstitial (Fig. 11A), with clusters associated with dilated tubules (Fig. 11B), muscular arteries, and the periglomerular interstitium. Tubular epithelial and glomerular staining were not detected at any time. No signal was seen in the LUO

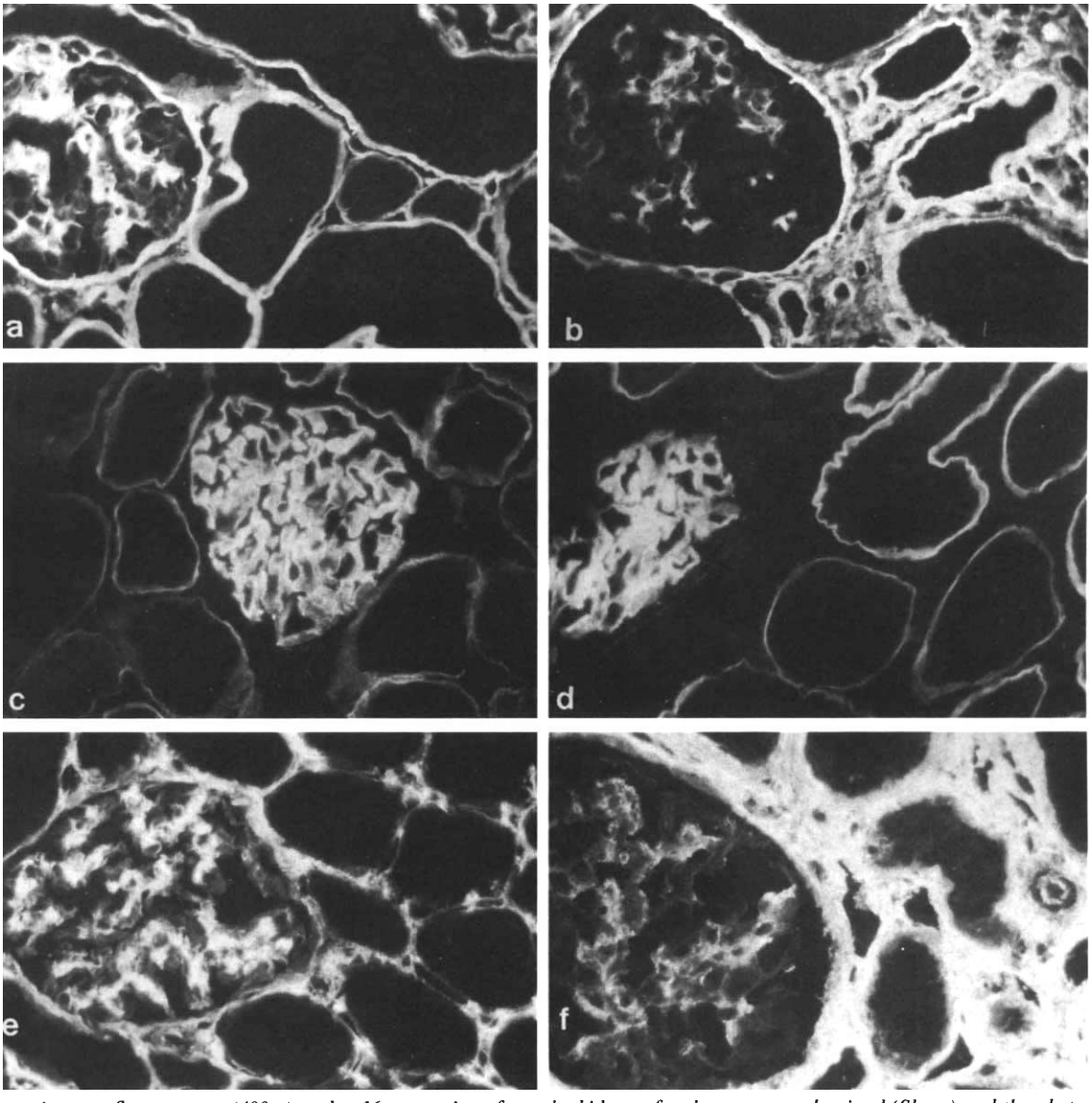

Fig. 7. *Indirect immunofluorescence (400×) at day 16 on sections from the kidney of a sham-operated animal (Sham) and the obstructed kidney (LUO) with (i) an antisera recognizing the non-collagenous globular domain of α2 (IV) collagen and confirming the presence of classical collagen IV in the interstitial space (**A** = Sham; **B** = LUO); (ii) a monoclonal antibody recognizing the α3 (IV) chain and demonstrating no interstitial reactivity for this novel collagen IV (**C** = Sham; **D** = LUO); and (iii) a polyclonal antisera reactive against rabbit fibronectin demonstrating increased interstitial fibronectin (**E** = Sham; **F** = LUO).*

cortex hybridized with the sense riboprobe (Fig. 11C) or in the CLK kidney hybridized with the antisense probe (Fig. 11D).

Hybridization with the antisense α1(IV) riboprobe localized expression of this mRNA in the LUO cortex to interstitial cells in a more diffuse pattern than was noted for α1(I) (Fig. 12A). Weak reactivity was occasionally noted in tubular epithelial cells. No signal was detected in the CLK cortex hybridized with the antisense riboprobe (Fig. 12C) or in either kidney with the sense riboprobe (Fig. 12B).

Discussion

Complete and irreversible loss of renal function follows within as little as 42 days of ureteral obstruction in the canine model [30]. In the rabbit complete obstruction of 8 to 12 weeks will achieve a similar outcome [31], and inulin clearance is substantially reduced after reversal of as little as four weeks of ureteral obstruction [32]. Interstitial fibrosis, tubular basement membrane thickening, tubular dilation and epithelial cell atrophy are the characteristic ultrastructural features of obstructive nephropathy in hydronephrotic human kidneys [4]. A significant correlation exists between quantitative indices of epithelial cell atrophy and interstitial expansion [5]. Finally, there is an inverse correlation between interstitial expansion and glomerular filtration rate in a variety of human renal disorders [3].

Analogous changes in the renal cortical tubular basement membrane and the interstitial space have previously been described in the rabbit model of UUO [7]. As confirmed here, these changes develop rapidly, with interstitial fibrosis, marked

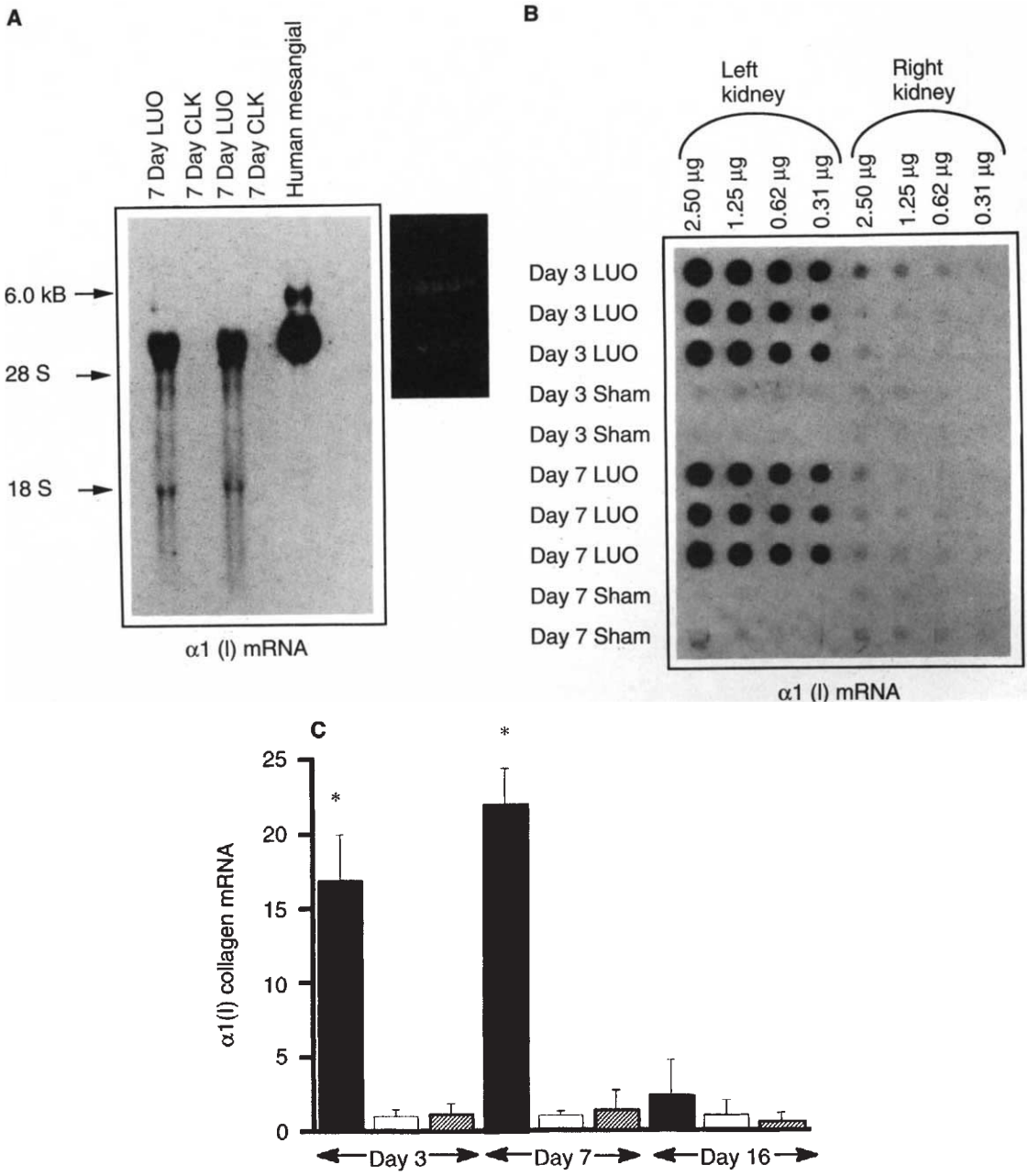

Fig. 8. *(A) Northern blot demonstrating specificity of α1(I) cDNA probe on total cortical RNA from two rabbits with LUO.* Total cellular RNA from human mesangial cells was used as a positive control. Inset in the upper right corner shows ethidium bromide stained gel with equal amounts of undegraded RNA. LUO = left ureteral obstruction, CLK = contralateral kidney. **(B)** RNA dot blot with α1(I) cDNA probe on RNA isolated from renal cortex of animals sacrificed 3 and 7 days after initial surgery. At each time, RNA from 3 LUO (left kidney), 3 CLK (right kidney) and 4 kidneys from sham-operated animals (Sham) was blotted at 2.5, 1.25, 0.6 and 0.3 μg serial dilutions. Following autoradiography, the membranes were re-probed with a cDNA probe encoding the 28S ribosomal RNA. **(C)** α1(I) mRNA content at day 3, 7 and 16 (mean ± 1 SD). For each sample, α1(I) mRNA was normalized to expression of the 28S ribosomal RNA to control for loading errors. In each group, values of the CLK were normalized to 1.0. Significant group differences were present at both days 3 and 7 (ANOVA $P < 0.0001$). In the LUO, mRNA content was significantly different from both the CLK and Sham groups ($P < 0.0001$ by PLSD). Sham and CLK values did not differ. Symbols are: solid bars, LUO; open bars, CLK; hatched bars, Sham; * $P < 0.0001$.

interstitial expansion and ultrastructural evidence of focal tubular basement membrane laminations visible by day 16 of UUO. Nagle and Bulger, in their original description of this model, reported that papillary necrosis was invariably present in the obstructed kidney [7]. Since this is rare in hydronephrotic human kidneys, they concluded that a unique feature of the rabbit papillary microcirculation predisposed to papillary necrosis. We confirmed this observation and thus deliberately excluded the medulla from our analysis.

Cortical interstitial fibrosis develops rapidly following UUO, although a similar chronology has been described for the rabbit model of crescentic nephritis accompanying anti-GBM disease

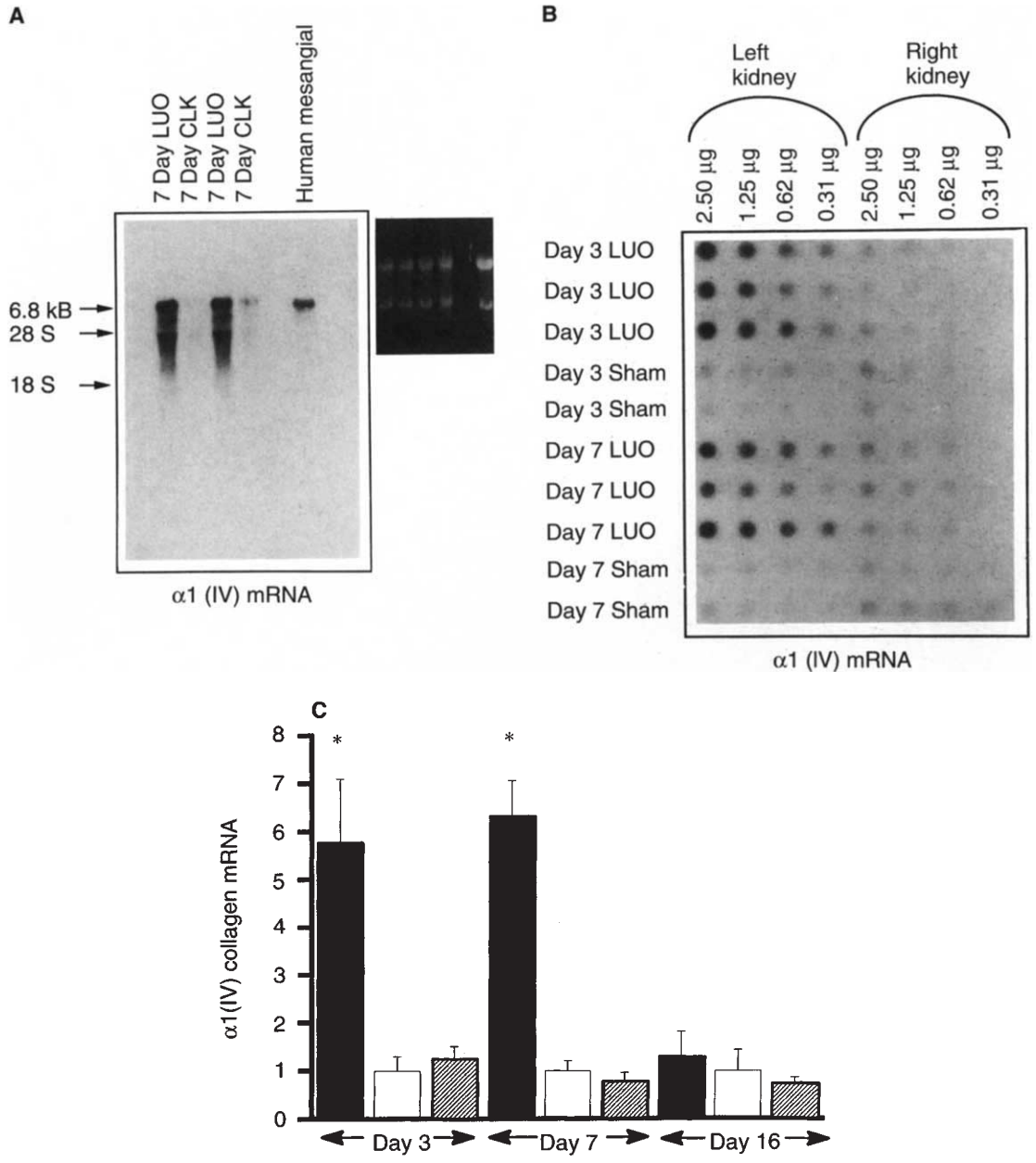

Fig. 9. *(A) Northern blot demonstrating specificity of α1(IV) cDNA probe on total cortical RNA from two rabbits with LUO.* Total cellular RNA from human mesangial cells was used as a positive control. Inset in the upper right corner shows ethidium bromide stained gel with equal amounts of undegraded RNA. LUO = left ureteral obstruction, CLK = contralateral kidney. **(B)** RNA dot blot with α1(IV) cDNA probe on RNA isolated from renal cortex of animals sacrificed 3 and 7 days after initial surgery. At each time, RNA from 3 LUO (left kidney), 3 CLK (right kidney) and 4 kidneys from sham-operated animals (Sham) was blotted at 2.5, 1.25, 0.6 and 0.3 μg serial dilutions. Following autoradiography, the membranes were re-probed with a cDNA probe encoding the 28S ribosomal RNA. **(C)** α1(IV) mRNA content at day 3, 7 and 16 (mean ± 1 SD). For each sample, α1(IV) mRNA was normalized to expression of the 28S ribosomal RNA to control for loading errors. In each group, values of the CLK were normalized to 1.0. Significant group differences were present at both days 3 and 7 (ANOVA $P < 0.0001$). In the LUO, mRNA content was significantly different from both the CLK and Sham values at days 3 and 7 ($P < 0.0001$ by PLSD). Sham and CLK values did not differ (P = NS). Symbols are: solid bars, LUO; open bars, CLK; hatched bars, Sham; * $P < 0.0001$.

[33, 34]. However, the evolution of changes in the rabbit UUO model appears to be more rapid than in most other models of interstitial fibrosis, including puromycin aminonucleoside (PAN) nephrosis [35, 36], cyclosporine toxicity [37], and murine systemic lupus erythematosis [38].

In addition to a diffuse increase in interstitial collagens I and III in the obstructed kidney, immunohistochemical studies demonstrated what appear to be focal, peritubular accumulations of these collagens encircling the TBM. Although it is difficult to distinguish between TBM reactivity and tightly packed interstitial collagen without immunoelectronmicroscopy, it is likely that this reflects tightly packed collagen in the

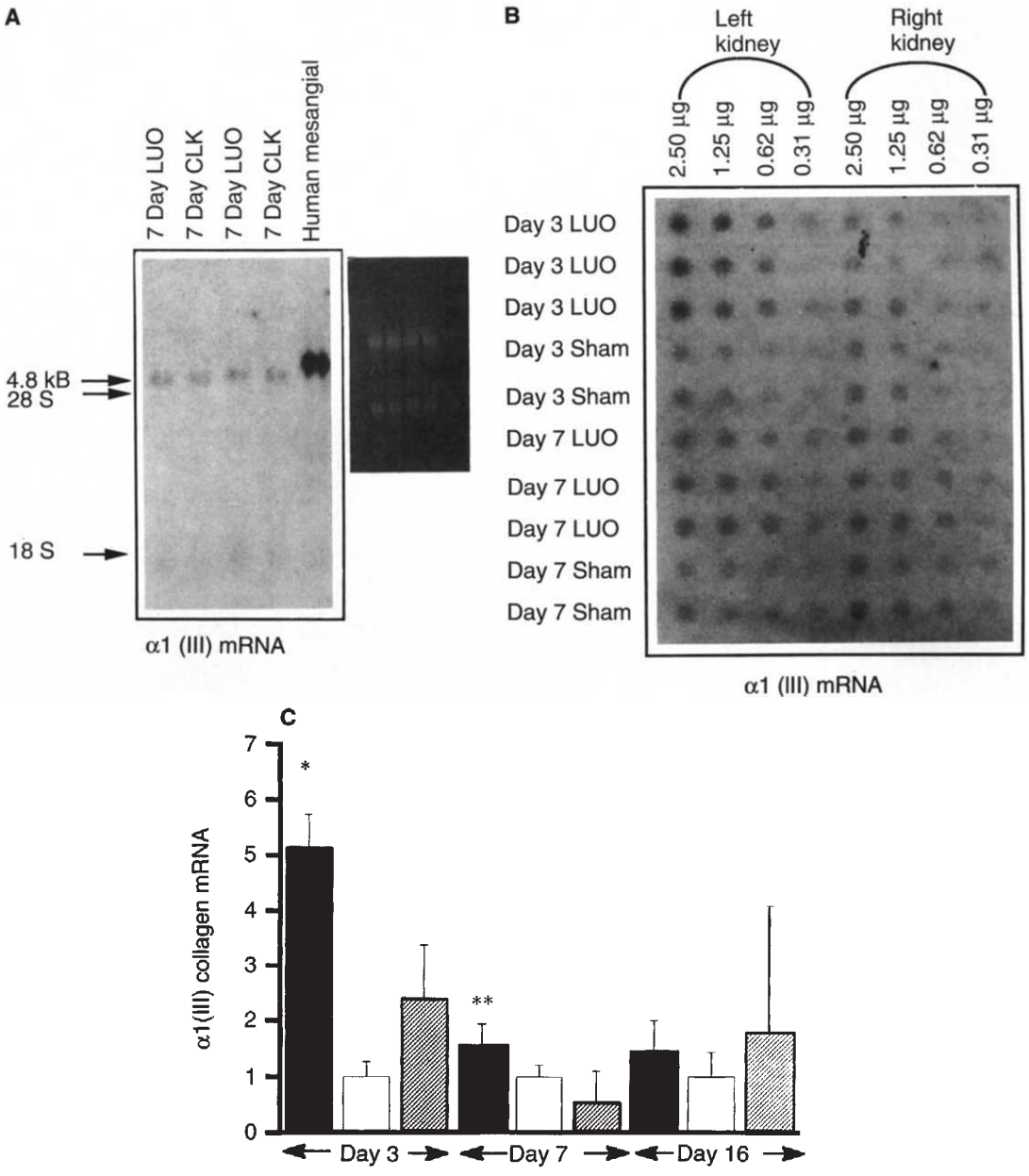

Fig. 10. *(A) Northern blot demonstrating specificity of α1(III) cDNA probe on total cortical RNA from two rabbits with LUO.* Total cellular RNA from human mesangial cells was used as a positive control. Inset in the upper right corner shows ethidium bromide stained gel with equal amounts of undegraded RNA. LUO = left ureteral obstruction, CLK = contralateral kidney. **(B)** RNA dot blot with α1(III) cDNA probe on RNA isolated from renal cortex of animals sacrificed 3 and 7 days after initial surgery. At each time, RNA from 3 LUO (left kidney), 3 CLK (right kidney) and 4 kidneys from sham-operated animals was blotted at 2.5, 1.25, 0.6 and 0.3 μg serial dilutions. Following autoradiography, the membranes were re-probed with a cDNA probe encoding the 28S ribosomal RNA. (C) α1(III) mRNA content at day 3, 7 and 16 (mean ± 1 SD). For each sample, α1(III) mRNA was normalized to expression of the 28S ribosomal RNA to control for loading errors. In each group, values of the CLK were normalized to 1.0. In the LUO, mRNA content was significantly different from both the CLK and Sham values at day 3 only (ANOVA $P < 0.001$; for the LUO vs. CLK, $P = 0.0002$; for the LUO vs. Sham, $P < 0.0002$; for the CLK vs. Sham, $P = 0.04$). At day 7, α1(III) expression was mildly elevated at 1.6 ± 0.4 times the CLK (ANOVA $P = 0.04$), and post-hoc testing localized this difference to the LUO vs. Sham comparison (for LUO vs. CLK, $P = 0.1$; for LUO vs. Sham, $P < 0.02$; for Sham vs. CLK, $P = 0.2$). At day 16, α1(III) expression was 1.5 ± 0.6 times the CLK, and this was not statistically significant (ANOVA $P = 0.8$). Symbols are: solid bars, LUO; open bars, CLK; hatched bars, Sham; * $P < 0.001$; ** $P < 0.05$.

peritubular interstitium. Although cultured NRK52E cells (a stable clone of rat tubular epithelial cells) can produce interstitial collagens *in vitro* [39], tubular epithelial cells are not widely believed to be capable of elaborating interstitial collagens *in vivo*. Our *in situ* hybridizations studies with riboprobes encoding α1(I) support this view, as tubular epithelial reactivity is consistently undetectable even in the obstructed kidney. Although lacking sensitivity for low abundance mRNA, these studies suggest that cells of the interstitial space, likely interstitial fibroblasts, may be responsible for increased collagen I

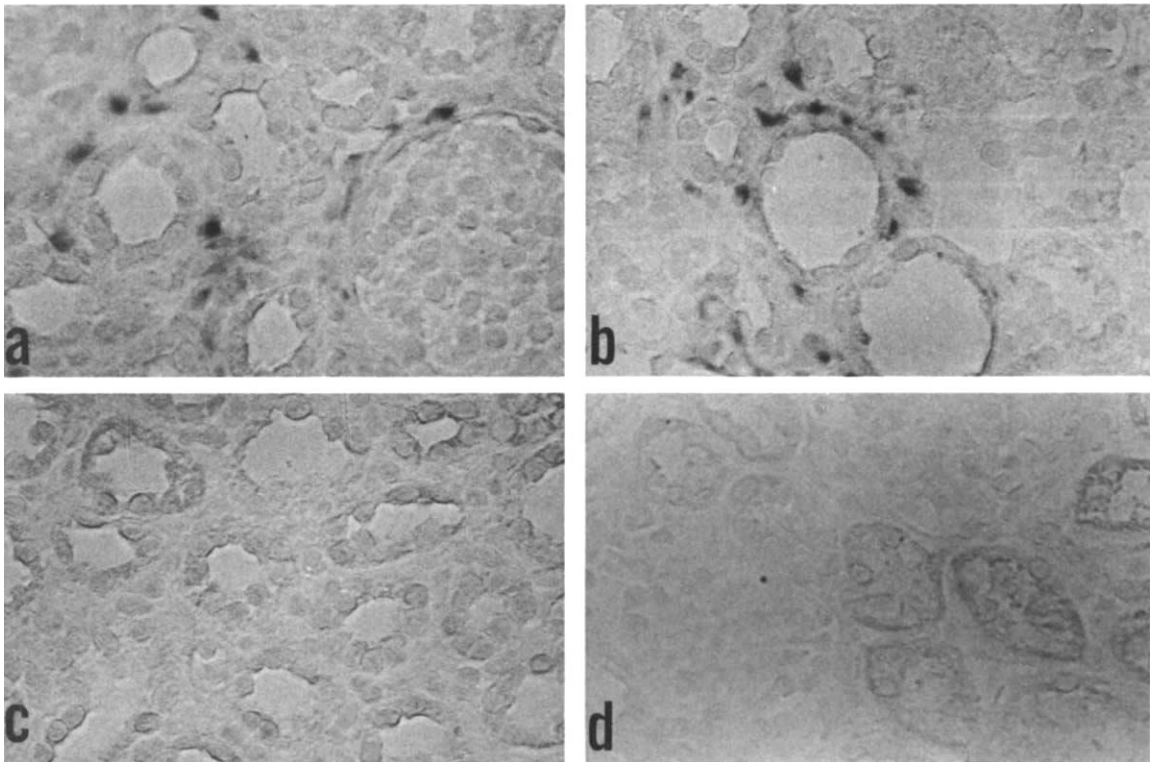

Fig. 11. In situ *hybridization was performed on cryostat sections of renal cortex from obstructed and contralateral kidneys from animals at day 7 following ureteral obstruction.* Sense and antisense riboprobes encoding α1(I) were labeled with digoxigenin-UTP and localized, after stringent washes, with an antidigoxigenin antiserum conjugated to alkaline phosphatase. The nitroblue tetrazolium color reaction yielded a purple-brown precipitate seen as a dark cytoplasmic stain. When cortical sections from the obstructed kidney were hybridized with the antisense riboprobe, reactive cells were exclusively interstitial **(A)**, with clusters associated with dilated tubules **(B)**, muscular arteries and glomeruli. No signal was detected when serial sections from the same kidney were hybridized with the sense riboprobe **(C)** or when the contralateral kidney was probed with the antisense riboprobe **(D)** (no counterstain, 500× magnification).

synthesis even when collagen I appears to be associated with TBMs. The apparent clustering of cells elaborating detectable α1(I) mRNA in the vicinity of muscular arteries, dilated tubules, and glomeruli suggests that increased ECM production in the cortical interstitium is not a homogenous process. This finding might explain the focal peritubular accumulation of collagens I and III described above. A similar distribution of α2(I) positive cells has been demonstrated by *in situ* hybridization in the rabbit model of anti-GBM disease, and it has been hypothesized that periarterial cells migrate from the adventitial space to contribute to interstitial fibrosis [40].

Increased staining for interstitial collagens I and III, fibronectin, TIN antigen, and heparan sulfate proteoglycan (Perlecan) appeared between days 3 and 7 of UUO in our model. Intriguingly, collagen IV becomes visible in the interstitium after as little as three days of UUO. This was confirmed using several antisera reactive with classical collagen IV [α1(IV) and α2(IV)]. The inability to demonstrate interstitial reactivity for novel collagen IV [α3 (IV)] suggests that the aberrant expression of collagen IV in the interstitium is selective for the classical collagen IV network. This is also the case in normal basement membranes where two separate, site-specific collagen IV networks have been proposed [41]. Thus, although UUO influences the dynamics of several important matrix proteins, the response to obstruction is a specific one.

The functional differences between the interstitial collagens I and III and basement membrane collagen IV are, in large measure, consequent to the extracellular modifications of the procollagen molecules. Collagens I and III undergo extracellular cleavage of their non-collagenous amino and carboxy terminii, which permits the rigid triple helices to align and form the characteristic striations of fibrillary collagen. In contrast, collagen IV retains the non-collagenous domains of the procollagen molecule, and these become sites of covalent interaction between adjacent molecules, producing the collagen IV lattice which provides mechanical strength and binding sites to all basement membranes [42]. The appearance of basement membrane collagen IV in the renal interstitium is not unique to this model and has been reported in both experimental and human interstitial disease [35, 43, 44], including a variety of end-stage kidney diseases in humans (unpublished observations). The results of our *in situ* hybridization studies suggest that the cells responsible for increased α1(IV) expression are predominantly interstitial, likely interstitial fibroblasts. Although cultured fibroblasts from other organs are known to express collagen IV mRNA [45], expression of functional protein product is often viewed as evidence for non-fibroblast lineage [46]. However, fibroblasts derived from human kidneys with interstitial fibrosis do elaborate collagen IV in culture [47]. Fibroblasts isolated from explants of hydronephrotic rabbit kidneys proliferate

more rapidly and have altered eicosanoid profiles when compared with CLK or normal rabbit kidneys, suggesting phenotypic differences which persist in cell culture [48]. Collagen IV production may be another expression of this altered phenotype.

Messenger RNA hybridization studies explored the processes underlying the accumulation of extracellular matrix proteins in the expanded interstitium and the TBM. The α1(I), α1(III) and α1(IV) collagen mRNAs were selected as representative interstitial and TBM matrix proteins. There was an increase in mRNA expression for each of these gene products to many times control values. Maximal expression occurred early in the course of LUO (between days 3 and 7) and thereafter returned towards control values. This suggests that a transient burst of matrix protein synthesis might account for the rapid evolution of interstitial fibrosis and TBM changes. Given the relative hypercellularity of the obstructed interstitium, it is not clear *a priori* whether increased matrix gene expression in total cortical RNA reflects activation of gene expression in individual cells or is merely a consequence of increased cell numbers. The *in situ* hybridization studies for α1(I) and α1(IV) clearly demonstrate that the mRNA content of individual cells is increased absolutely, as no signal could be detected in the unobstructed kidney examined under identical conditions.

Although mRNA content for specific ECM components tended to be greater in the LUO samples than in controls at day 16, these difference were not statistically significant. It is possible that these differences might have achieved significance if a larger group of animals were studied, but it is likely that changes of this magnitude are below the sensitivity of the currently available methodology to detect [49, 50] (assuming a power of 90%, more than 30 animals per group would be required to detect a twofold increase in α1(I) mRNA at day 16 with a P value < 0.05). In any case, our studies clearly describe the dynamics of a rapid increase and rapid subsequent decrease in mRNA encoding extracellular matrix components in the UUO model.

Several mechanisms may be operative for fibrosis to persist even as mRNA expression diminishes. First, as discussed above, mRNA expression could remain elevated but below the threshold of detectability of our studies. Second, post-transcriptional changes in translational efficiency or mRNA stability might increase collagen biosynthesis in the absence of changes in steady-state mRNA expression [51]. This has recently been implicated as a mechanism for IL-1 induced synthesis of α1(I) collagen in the absence of changes in mRNA expression in cultured Ito cells [52]. Third, there may also be reduced rates of matrix degradation. Thus, in the rat studied after 15 days of UUO, collagenolytic activity in renal cortical homogenates was depressed 8- to 10-fold in the obstructed kidney [53]. The demonstration of increased mRNA expression for the tissue inhibitor of the metalloproteases (TIMP) in the interstitial fibrosis which accompanies PAN nephrosis [35] is further support for this hypothesis.

In summary, this report demonstrating early and striking changes in the ECM composition of the interstitial space in the rabbit model of UUO, supports the view that interstitial fibrosis and TBM thickening are important early lesions in the pathogenesis of irreversible renal injury in obstructive nephropathy. The early increase in ECM mRNA content implicates increased matrix synthesis in the pathogenesis of this renal injury, and *in situ* hybridization localizes increased expression of collagens I and IV to the interstitial cell population of the obstructed kidney. The precise mechanism for this increased gene expression requires further study.

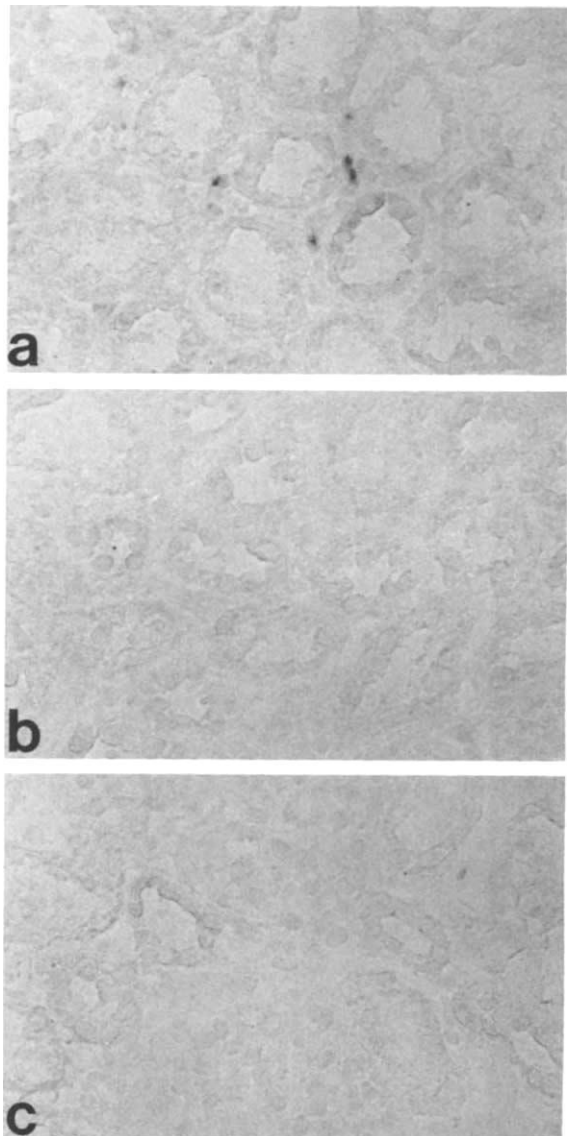

Fig. 12. In situ *hybridization was performed on cryostat sections of renal cortex as described in the legend of Fig. 11.* When cortical sections from the obstructed kidney were hybridized with a riboprobe antisense to the α1(IV) mRNA, signal was noted predominantly in interstitial cells (**A**), although weak reactivity was occasionally seen in tubular epithelial cells. No signal was detected when serial sections from the same kidney were hybridized with the sense riboprobe (**B**) or when the contralateral kidney was probed with the antisense riboprobe (**C**) (no counterstain, 500× magnification).

Acknowledgments

Dr. Sharma was supported by the Duncan L. Gordon Fellowship from the Hospital for Sick Children Foundation, Toronto, Canada. This work was supported by the Viking Children's Fund, Minneapolis, Minnesota, and N.I.H. grant AI 10704. The authors acknowledge the

technical assistance of Sylvia Rozen, Kim Pinkham, Kathy Divine, Mike Stenzel and Bill Tanner. Gifts of antisera and cDNA clones were provided by Drs. J. Weislander (Mab 17), A. Ljubimov (Mab A7L6), Y. Yamada (cDNA p1275) and I.G. Wool (cDNA 28S).

Reprint requests to Atul K. Sharma M.D., Montreal Children's Hospital, Room E.222, 2300 Rue Tupper, Montreal, Canada H4A 1P3.

References

1. Gonzalez R, Reinberg Y, Burke B, Wells T, Vernier RL: Early bladder outlet obstruction in fetal lambs induces renal dysplasia and the prune-belly syndrome. *J Pediatr Surg* 25:342–45, 1990
2. McEnery PT, Stablein DM, Arbus G, Tejani A: Renal transplantation in children: A report of the North American Pediatric Renal Transplant Cooperative Study. *N Engl J Med* 326:1727–1732, 1992
3. Bohle A, Mackensen-Haen S, Gise H, Grund KE, Wehrmann M, Batz C: The consequences of tubulo-interstitial changes for renal function in glomerulopathies: A morphometric and cytologic analysis, in *Tubulo-interstitial Nephropathies*, edited by Amerio A, Coratelli P, Massry SG, Norwell, Kluwer Academic Publishers, 1991, pp. 29–40
4. Moller JC, Skriver E, Olsen S, Maunsbauch AB: Ultrastructural analysis of human proximal tubules and cortical interstitium in chronic renal disease (hydronephrosis). *Virchows Arch* (Pathol Anat) 402:209–237, 1984
5. Moller JC, Skriver E: Quantitative ultrastructure of human proximal tubules and cortical interstitium in chronic renal disease (hydronephrosis). *Virchows Arch* (Pathol Anat) 406:389–406, 1985
6. Nagle RB, Bulger RE, Cutler RE, Jervis HR, Benditt EP: Unilateral obstructive nephropathy. I. Early morphologic, physiologic, and histochemical changes. *Lab Invest* 28:456–467, 1973
7. Nagle RB, Bulger RE: Unilateral obstructive nephropathy in the rabbit. II. Late morphologic changes. *Lab Invest* 38:270–78, 1978
8. Lane PH, Steffes MW, Fioretto P, Mauer SM: Renal interstitial expansion in insulin-dependent diabetes mellitus. *Kidney Int* 43:661–667, 1993
9. Kim Y, Butkowski R, Burke B, Kleppel MM, Crosson J, Katz A, Michael AF: Differential expression of basement membrane collagen in membranous nephropathy. *Am J Pathol* 139:1381–1388, 1991
10. Lemley KV, Kriz W: Anatomy of the renal interstitium. *Kidney Int* 39:370–381, 1991
11. Weber M: Basement membrane proteins. *Kidney Int* 41:620–628, 1992
12. Platt JL, Michael AF: Retardation of fading and enhancement of intensity of immunofluorescence by p-phenylenediamine. *J Histochem Cytochem* 31:840–842, 1983
13. Chomcynzki P, Sacchi N: Single-step method of RNA isolation by acid guanidinium thiocyanate-phenol-chloroform extraction. *Anal Biochem* 162:156–159, 1987
14. Chu ML, Myers JC, Bernard MP, Ding JF, Ramirez F: Cloning and characterization of five overlapping cDNAs specific for the human pro α1(I) collagen chain. *Nucl Acid Res* 10:5925–5934, 1982
15. Chu ML, Weil D, de Wet W, Bernard M, Sippola M, Ramirez F: Isolation of cDNA and genomic clones encoding human pro-α1(III) collagen: Partial characterization of the 3′ end region of the gene. *J Biol Chem* 260:4357–4363, 1985
16. Oberbaumer I, Laurent M, Schwarz U, Sakurai Y, Yamada Y, Vogeli G, Voss T, Siebold B, Glanville RW, Kuhn K: Amino acid sequence of the non-collagenous globular domain (NC1) of the alpha 1(IV) chain of basement membrane collagen as derived from complementary DNA. *Eur J Biochem* 147:217–224, 1985
17. Correa-Rotter R, Mariash CN, Rosenberg ME: Loading and transfer control for northern hybridization. *Biotechniques* 12:154–158, 1992
18. Kolbe M, Kaufman JL, Friedman J, Dinerstein C, MacKenzie JW, Boyd CD: Changes in steady-state levels of mRNAs coding for type IV collagen, laminin and fibronectin following capillary basement membrane thickening in human adult onset diabetes. *Connect Tissue Res* 25:77–85, 1990
19. Fogel MA, Boyd CD, Leardkamolkarn V, Abrahamson DR, Minto WM, Salant DJ: Glomerular basement membrane expansion in passive Heymann nephritis: Absence of increased synthesis of type IV collagen, laminin or fibronectin. *Am J Pathol* 138:465–475, 1991
20. Chan YL, Olvera J, Wool IG: The structure of rat 28S ribosomal ribonucleic acid inferred from the sequence of nucleotides in a gene. *Nucl Acid Res* 11:7819–7831, 1983
21. Yamaguchi N, Sato N, Ko JS, Ninomiya Y: Cloning of α1(IV) and α2(IV) collagen cDNAs from rabbit corneal endothelial cell RNA. *Invest Ophthalmol Vis Sci* 32:2924–2930, 1991
22. Cox KH, DeLeon DV, Angerer LM, Angerer RC: Detection of mRNAs in sea urchin embryos by *in situ* hybridization using asymmetric RNA probes. *Develop Biol* 101:485–502, 1984
23. Foellmer HG, Madri JA, Furthmayr H: Monoclonal antibodies to type IV collagen: Probes for the study of structure and function of basement membranes. *Lab Invest* 48:639–649, 1983
24. Butkowski RJ, Wieslander J, Kleppel M, Michael AF, Fish AJ: Basement membrane collagen in the kidney: Regional localization of novel chains related to collagen IV. *Kidney Int* 35:1195–1202, 1989
25. Kleppel MM, Santi PA, Cameron JD, Wieslander J, Michael AF: Human tissue distribution of novel basement membrane collagen. *Am J Pathol* 134:813–825, 1989
26. Engvall E, Earwicker D, Haaparanta T, Ruoslahti E, Sanes JR: Distribution and isolation of four laminin variants; tissue restricted distribution of heterotrimers assembled from five different subunits. *Cell Reg* 1:731–740, 1989
27. Couchman JR, Ljubimov AV: Mammalian tissue distribution of large heparan sulfate proteoglycan detected by monoclonal antibodies. *Matrix* 9:311–321, 1989
28. Katz A, Fish AJ, Kleppel MM, Hagen SG, Michael AF, Butkowski RJ: Renal entactin (nidogen): Isolation, characterization and tissue distribution. *Kidney Int* 40:643–652, 1991
29. Butkowski RJ, Kleppel MM, Katz A, Michael AF, Fish AJ: Distribution of tubulointerstitial nephritis antigen and evidence for multiple forms. *Kidney Int* 40:836–846, 1991
30. Vaughan ED, Gillenwater JY: Recovery following complete chronic unilateral ureteral occlusion. *J Urol* 106:27–35, 1971
31. Soer JR: Temporary obstruction of the ureter: An experimental study of the recovery of renal function after reversible obstruction of the ureter in the rabbit. *Arch Chir Neerl* 26:77–86, 1974
32. Kinn AC, Bohman SO: Renal structural and functional changes after unilateral ureteral obstruction. *Scan J Urol Nephrol* 17:223–234, 1983
33. Downer G, Phan SH, Wiggins RC: Analysis of renal fibrosis in a rabbit model of crescentic nephritis. *J Clin Invest* 82:998–1006, 1988
34. Merritt SE, Killen PD, Phan SH, Wiggins RC: Analysis of α1 (I) procollagen, α1 (IV) collagen, and β-actin mRNA in glomerulus and cortex of rabbits with experimental glomerular basement membrane disease: Evidence for early extraglomerular collagen biosynthesis. *Lab Invest* 63:762–769, 1990
35. Jones CL, Buch S, Post M, McCulloch L, Liu E, Eddy AA: Pathogenesis of interstitial fibrosis in chronic purine aminonucleoside nephrosis. *Kidney Int* 40:1020–1031, 1991
36. Nakamura T, Ebihara I, Fukui M, Tomino Y, Koide H: Effects of methylprednisolone on glomerular and medullary mRNA levels for extracellular matrices in puromycin aminonucleoside nephrosis. *Kidney Int* 40:874–881, 1991
37. Nast CC, Adler SG, Artishevsky A, Kresser CT, Ahmed K, Anderson PS: Cyclosporine induces elevated procollagen α1 (I) mRNA levels in the rat renal cortex. *Kidney Int* 39:631–638, 1991
38. Nakamura T, Ebihara I, Shirato I, Tomino Y, Koide H: Increased steady-state levels of mRNA coding for extracellular matrix components in kidneys of NZB/W F1 mice. *Am J Pathol* 139:437–450, 1991
39. Creely JJ, DiMari SJ, Howe AM, Haralson MA: Effects of transforming growth factor-β on collagen synthesis by normal rat kidney epithelial cells. *Am J Pathol* 140:45–55, 1992
40. Wiggins RC, Goyal M, Merritt SE, Killen PD: Localization of α2 (I) collagen mRNA by *in situ* hybridization to the periarterial and

periglomerular regions in anti-GBM crescentic nephritis (abstract). *J Am Soc Nephrol* 2:568, 1991
41. KLEPPEL MM, FAN WW, CHEONG HI, MICHAEL AF: Evidence for separate networks of classical and novel basement membrane collagen: Characterization of α3 (IV)-Alport antigen heterodimer. *J Biol Chem* 267:4137–4142, 1992
42. VAN DER REST M, GARRONE R: Collagen family of proteins. *FASEB J* 5:2814–2823, 1991
43. KASHTAN CE, KIM Y: Distribution of the α1 and α2 chains of collagen IV and of collagens V and VI in Alport syndrome. *Kidney Int* 42:115–126, 1992
44. EBIHARA I, KILLEN PD, LAURIE G, HUANG T, YAMADA Y, MARTIN GR, BROWN KS: Altered mRNA expression of basement membrane components in a murine model of polycystic kidney disease. *Lab Invest* 58:262–269, 1988
45. LANKAT-BUTTGEREIT B, KUOLZIK M, HUNZELMANN N, KRIEG T: Cytokines alter mRNA steady-state levels for basement membrane proteins in human skin fibroblasts. *J Dermatol Sci* 2:300–307, 1991
46. PERKINS S, FLEISCHMAN RA: Stromal cell progeny of murine bone marrow fibroblast colony forming units are clonal endothelial-like cells that express collagen IV and laminin. *Blood* 75:620–625, 1990
47. MÜLLER GA, RODEMANN P: Characterization of human renal fibroblasts in health and disease: Immunophenotyping of cultured tubular epithelial cells and fibroblasts derived from kidneys with histologically proven interstitial fibrosis. *Am J Kidney Dis* 17:680–683, 1991
48. DAVIS BB, THOMASSON D, ZENSER TV: Renal disease profoundly alters cortical interstitial cell function. *Kidney Int* 23:458–464, 1983
49. DE LEEUW WJF, SLAGBOOM PE, VIJG J: Quantitative comparison of mRNA levels in mammalian tissues: 28S ribosomal RNA level as an accurate internal control. *Nucl Acid Res* 17:10137–10138, 1989
50. VOLKENANDT M, DICKER AP, BANERJEE D, FANIN R, SCHWEITZER B, HORIKOSHI T, DANENBERG K, DANENBERG P, BERTING JR: Quantitation of gene copy number and mRNA using the polymerase chain reaction. *PSEBM* 200:1–6, 1992
51. CARTER BZ, MALTER JS: Biology of disease: Regulation of mRNA stability and its relevance to disease. *Lab Invest* 65:610–621, 1991
52. ARMENDARIZ-BORUNDA J, KATAYAMA K, SEYERS JM: Transcriptional mechanisms of type I collagen gene expression are differentially regulated by interleukin-1β, tumor necrosis factor α, and transforming growth factor β in Ito cells. *J Biol Chem* 267:14316–14321, 1992
53. GONZÁLEZ-AVILA G, VADILLO-ORTEGA F, PÉREZ-TAMAYO R: Experimental diffuse interstitial fibrosis: A biochemical approach. *Lab Invest* 59:245–252, 1988